2

Thermodynamic Phenomena in Glass

2.1 Binding Enthalpy

Whatever method – mechanical, thermal or chemical – we use, microstructuring of glasses is always intrusive, which means bonds between anions and cations are being broken, and this requires energy. The actual energy required for the process of microstructuring has to exceed the theoretical binding energy and must also cover the needs for the applied process conditions and losses.

Section 1.1 describes the ionic arrangement and structure of glasses. The presence of short-range order, as represented in the structure coordination tetrahedra, but absence of long-range ordering, which results in the random arrangement of the coordination polyhedra in the glassy network, makes it rather difficult to formulate generally valid statements about energetic phenomena in glasses. If we indeed want to define a certain value for the binding energy even for a glass with a well-defined composition, we have to consider that this would only represent a mean value with a wide distribution.

From a practical point of view, only processes operating at constant pressure are of interest for glass microstructuring. Therefore, we should not use the term "energy" to describe energetic phenomena in the glassy network. It is better to use enthalpy (2.1):

$$H = U + pV \tag{2.1}$$

where H is the enthalpy, U the internal energy, p the pressure and V the specific volume.

The Gibbs–Helmholtz equation links the enthalpy H with the (Gibbs) free enthalpy G which is the available energy in chemical systems at a given absolute temperature (2.2)

$$\Delta G = \Delta H - T\Delta S \tag{2.2}$$

where S is the entropy.

Table 2.1. Thermophysical parameters of some common glasses [261]

Glass	Enthalpy $\Delta_b H^o$ at standard conditions (kJ mol^{-1})	Entropy $\Delta_b S^o$ at standard conditions (J mol^{-1} K^{-1})
Sodium calcium silicate	−810	45.6
Pyrex	−1080	44.0
Fused silica	−908	43.4

Both, enthalpy and entropy at standard conditions for chemical elements and compounds are tabularised [50]. Using these values Jacquorie [261] calculated H and S at standard conditions for a sodium calcium silicate, a sodium borosilicate and a pure silica glass (Table 2.1).

These actual values of H, S and G depend on the actual temperature (2.3) and (2.4) and affect as a consequence the free enthalpy G (2.5):

$$H_{(T)} = H_0 + \int_0^T C_p \, \mathrm{d}T, \tag{2.3}$$

$$S_{(T)} = \int_0^T \frac{C_p}{T} \, dT \tag{2.4}$$

$$G_{(\mathrm{T})} = H_0 + \int_0^T C_p \, \mathrm{d}T - T \int_0^T \frac{C_p}{T} \, \mathrm{d}T \tag{2.5}$$

where C_p is the specific heat at constant pressure and H_0 the enthalpy at standard conditions.

These energetic parameters are valid for one mole of a given glass composition and represent an integrated median value over all types of bonds in the glassy network. These values do not provide accurate information about the binding enthalpy between for instance oxygen and silicon in a glass, because it cannot be distinguished whether the oxygen is bridging or a nonbridging. If the oxygen is nonbridging the bond is heteropolar and requires the presence of another cation in the vicinity, which also affects the strength of the neighbouring bond between oxygen and silicon. A value for the Si–O–Si binding enthalpy does not contain any information about the binding enthalpy between O^{2-} and the other cation. Therefore, in order to estimate the binding enthalpy between special anions and cations, the problem reduces frequently to a comparison of the differences in the electrical field strength ((1.1) and Table 1.1).

More than 50 years ago, Sun [508] defined the chemical binding energy B of a given glass composition (2.6) using the exact chemical composition (mol%), the energy D required for dividing/dissociating the oxides, which are represented in the form RO_y where $y = n/m$ in R_mO_n, into their atoms in

the gaseous state as well as the coordination numbers CN (see Sect. 1.1) of the cations in the oxides.

$$B = \sum_{i=1}^{n} \frac{D_i}{CN_i} \tag{2.6}$$

Surprisingly, for most studied glass compositions the value B is very close to 420 kJ mol^{-1}. Perhaps this value could offer a clue to understand energy, which is theoretically required for microstructuring glasses. The actual energy value that is required for the process, however, must include the additional kinetic energy contributions, as well as those required to overcome the energy which is holding all the ions in exact positions, with fixed distances and angles. It follows that all processes to microstructure glasses have to overcome an initial activation energy and require energy for removing the ions from their original position (that means for transportations).

2.2 Mechanisms of Materials Transport in Amorphous Homogeneous Solids

2.2.1 Viscous Flow

The temperature dependence of viscosity of a soda lime silicate glass (Fig. 1.11) was already discussed previously and its relevance to glass processing, especially to obtain stress-free glass products was also explained. The viscoelastic behaviour of glasses can be described by Newton's (1.2) and Maxwell's law (1.4). Very comprehensive reviews of the subject matter have been published by Scholze [450] and Brückner et al. [74]. Pye et al. [414] give tables which allow for calculation the viscosity of glass melts in dependence on composition and temperature.

During the process of microstructuring, glasses are often exposed to elevated temperatures, which is true in the case of laser treatments and modified UV-supported lithography. Viscous flow occurs if the applied temperatures exceed the transformation temperature T_g of the glass (Sect. 1.1.4). The glass is especially susceptible to viscous flow at the edges of micrometer-sized holes and channels, if the stress driven by the surface tension γ of the glass (melt) acts towards the bulk of the device. Microstructured edges will deform easily if surface tension stress is high, the viscosity low and the residence time at elevated temperatures long enough. In order to be able to estimate the impact of viscous flow on the final appearance of the microstructured device it would be helpful to be able to describe the flow process at the atomic level.

A glass melt, just as the solidified glass itself, does not possess as explained before any long-range ordering. If a melt is sheared what forces it to flow, then initially the bond angles between the polyhedra will change and bonds are stretched up to a point at which eventually the chemical bonds will break. Thermal and mechanical energy is required to heating the glass, to interrupt

the chemical bonds and eventually to overcome attractive Coulomb interactions and finally to allow the ions, polyhedra or clusters to move freely, which depends on temperature and applied shear stress.

Broken bonds, but not the same, immediately reform again after the melt experienced some deformation. The reformation of bonds leads to a recovery of chemical binding energy. This process is repeated as long as stress is applied. Thermal energy is only required to break the chemical bonds and to overcome attractive Coulomb interactions, but the glass melt starts to flow because of applied external stress acting on the glass or because of surface tension gradients. The temperature dependence of the viscosity of glass melts can be described by or fitted to an Arrhenius expression (2.7):

$$\eta = \eta_0 \exp\,(E_\eta/RT), \tag{2.7}$$

where η is the viscosity, η_0 a constant, E_η the activation energy that must be overcome to induce viscous flow, R is the gas constant and T the absolute temperature in K. The so-called Arrhenius plot log η vs. $1/T$ should result in a straight line. This would be the case if E_η would be a constant, which is rarely observed. In most cases, Arrhenian behaviour is only observed at very high temperatures where melts are very fluid or near the glass transformation range. However, E_η is very much smaller for fluid melts than for high viscosity melts near the glass transformation range. In the range between the limiting Arrhenius regions, E_η is a function of temperature. Avramov [13] determined the activation energy from the slope of the Arrhenius plot of viscosity against the reciprocal temperature and discussed the results near the transformation temperature. A typical Arrhenius plot for soda lime silicate glass is shown in Fig. 2.1. The slope of this curve, i.e. the activation energy, at temperatures

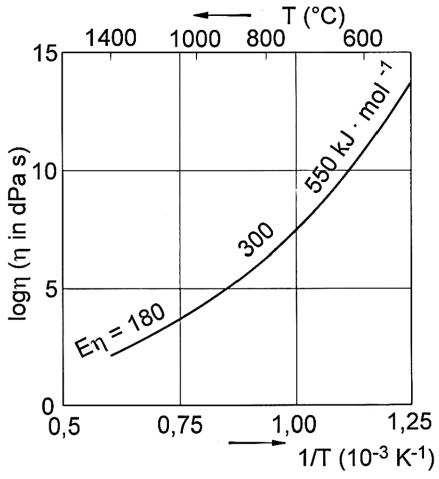

Fig. 2.1. Arrhenius plot lg $\eta = f(1/T)$ for a soda lime silicate glass in the temperature range above the glass transformation (original data see Fig. 1.11)

above T_g is relatively large (550 kJ mol^{-1}), but it still allows for deformations to occur. It is important for thermal bonding of different glasses to each other or between microstructured glass wafers to silicon (anodic bonding). In the first case the bonding temperature must not exceed the annealing temperature (a higher temperature would indeed favour the desired diffusion between both glass devices, but simultaneously the undesired deformation of the microstructures) and in the second case it has to remain below the strain point in order to avoid diffusion processes in the doped silicon wafers.

Viscous flow in microstructured glass devices, which is responsible for the rounding of edges and the deformation of walls, occurs during the postcrystallisation of UV-sensitive devices which is performed to improve their mechanical properties (see Sect. 1.2.4). Certain technical provisions are required to prevent the undesired deformation of glass devices.

2.2.2 Diffusion

Diffusion describes the movement of atoms, molecules or ions through matter, i.e. gases, fluids or solids. Diffusion is their movement driven by a concentration gradient from a region of higher concentration (or chemical potential) to lower concentration, which gives the process directionality. Any type of fields/gradients, such as mechanical stresses, temperature gradients, magnetic and electric fields, can also influence the direction of diffusion. Chemical, thermal or mechanical gradients are the most common drivers for diffusion in microstructured glasses. The kinetic energy of the diffusing species increases exponentially with temperature. Diffusion coefficients behave in a similar manner, i.e. diffusion processes in glasses can be neglected at room temperature but become significantly at temperatures in the glass transition range and above it. Diffusion is a thermally activated process, so the temperature dependence of diffusion coefficients can be described by means of an Arrhenius expression (2.8) which holds at temperatures $T > T_g$:

$$D(T) = D_0 \exp\left(\frac{-E_D}{RT}\right), \tag{2.8}$$

where $D(T)$ is the diffusion coefficient of a species at a given temperature, D_0 is pre-exponential diffusion constant at standard conditions, E_D is the activation energy for diffusion to occur and R the gas constant. The diffusion constant D_0 depends on the underlying diffusion mechanism and the diffusing species; i.e. atoms, molecules, ions or ionic clusters. The diffusion of charged species is affected by electrostatic interaction between the species and the surrounding matter. Therefore it is not the same if e.g. silver or oxygen exists in a glass as atoms or ions. Experimental diffusion coefficients of ions represent only mean values. The values can vary by an order of magnitude even for supposedly identical glasses, which is due to real differences in the glasses because of the absence of any long range order. Diffusion coefficients

of individual ions depend strongly on the valency and the radius of the ion but also on the surrounding matter. It is impossible to predict diffusion coefficients of ions, such as Na^+, K^+ and Ca^{2+}, in a glass without providing any information about the glass composition. Ions diffuse only remarkably at temperatures exceeding the glass transformation temperature. The diffusion in bulk glasses of ions (or atoms) takes place utilising interruptions and interstices in rings formed by the silica tetrahedra. Ion diffusion may occur via self- or interdiffusion. Self-diffusion is the diffusion of an ion which is the primary component of the glass whereas interdiffusion or ion exchange occurs when a glass containing a certain mobile ion is in contact with a source of a different mobile ion (e.g. from molten salt). This process is of significant interest for many technical applications. If the diffusing ionic species have different sizes, it also means that mobility in the glass is different, which causes differences in the diffusion rates of these ions, and that will result in the development of a temporary electric field in the glass. This field, on the one hand, will slow down the diffusion of the faster ion but, on the other hand, will accelerate the diffusion of the slower ion until the diffusion rates are equalised.

The interdiffusion process between glass containing a mobile ion, such as K^+, in contact with a source of different mobile ions with a valency, such as Ca^{2+}, requires that two K^+ diffuse per one diffusing Ca^{2+} ion because of electroneutrality reasons. However, if we recall what we learned about coordination numbers (see Sect. 1.1), we understand that such an ion-exchange process rarely takes place. However, an ion exchange between various monovalent ions, such Li^+, Na^+ and K^+, is often used to modify for instance near surface properties of glasses or to strengthen glasses. The ion radii of various monovalent ions vary significantly (see Table 1.1), which determines their space requirements in a glass, i.e. larger ions require larger interstices in the tetrahedra rings. Interdiffusing K^+, having a large mass, leads to an increased optical density and, therefore, increased refractive index (see also Fig. 1.51). If a K^+ is exchanged for a smaller ion, which can occupy smaller interstices, this causes significant compressive stresses near the surface region.

Most commercial ion exchange processes take place by exposing a (microstructured) glass device to a bath containing the melt of suitable salt. The diffusion (ion exchanging) temperature has a major influence on the final result. At $T > T_g$ additionally viscous flow processes might occur which lead to the deformation of the rings of tetrahedra. Whereas at $T < T_g$ the interdiffusion of large cations into the glass containing smaller primary ions causes compressive stress which influences the optical and mechanical properties of glass devices, however, an ion exchange at $T > T_g$ causes flowing and will affect the thermal expansion coefficient in the outer devices layers, which will again influence the refractive indexes and mechanical stresses, but in a different way as at $T < T_g$. As described in Sect. 1.2.4, it is possible to produce light guiding paths in microstructured glass springs [201] by ion exchange process but also to improve the mechanical strength of glasses by the compressive stresses arising form ion exchange [338]. An ion exchange by interdiffusion

Table 2.2. Interdiffusion coefficient $D_{Na^+ \leftrightarrow Li^+}$ as a function of temperature for FS 21 glass [201]

T(°C)	$D_{Na^+ \leftrightarrow Li^+}$ (10^{-10} cm^2 s^{-1})
320	2.12
340	3.21
360	5.00
380	12.99
400	17.58

below the strain point of the glass will guarantee that the diffusion process is not accompanied by a deformation of the glass device. Hecht-Mijic [201] measured and calculated the interdiffusion coefficients (Table 2.2) for an exchange of Na^+ against Li^+ in FS21 glass in a $NaNO_3$-melt as function of temperature.

This exchange process of Na^+ against Li^+ in FS21 can be described by an Arrhenius expression up to the strain point of FS21 at 383°C and again at $T > T_U$, however now having a different slope. This behaviour signalises a strong correlation between the transport mechanisms in glasses by viscous flow and diffusion.

Baumgart [25] investigated almost the same glass composition as Hecht-Mijic [201]. However, the silver dopand was introduced into the glass via an ion exchange in an $Ag/NaNO_3$ melt. The measured and calculated diffusion coefficients at 405°C are shown in Table 9.4. In this case the diffusion rate of Ag^+ controls the ion exchange rate. The diffusion profiles can be described by Fick's laws (2.9) and (2.10):

$$j = \frac{\mathrm{d}N}{A\mathrm{d}t} = -D_o \frac{\delta c}{\delta x} \frac{1}{V}, \tag{2.9}$$

$$\frac{\delta c}{\delta t} = D_o \frac{\delta^2 c}{\delta x^2}, \tag{2.10}$$

where j is flux of the diffusing species, i.e. the number of species diffusing from a given volume in 1 s through an area of 1 cm^2, N is the number of diffusing species, A the area, V the volume, t the time, D_o the diffusion constant, $\delta c/\delta x$ is the concentration gradient of the diffusing species in the direction x.

The ion exchange process occurring between the salt melt and the glass surface is determined by the composition/concentration gradient across the surface, the chosen temperature and the diffusion time. The diffusion rate is controlled by the larger, i.e. slower diffusing ion.

The growth of LMS crystals around Ag-nuclei in photosensitive glasses, as described in Sect. 1.2.4, is also a diffusion process. The Ag particles are homogeneously distributed throughout the glass (matrix and droplets, see Fig. 1.39 and Mrotzek [365]), however, only the Ag clusters in the droplets become nuclei for the growth of Li_2O. SiO_2 crystals (LMS) because the chemical composition of the droplets is similar to that of LMS and, therefore, the

diffusion distances are short. The equations describing the nucleation (2.18) and crystal growth process (2.19) account for the importance of the diffusion via the inclusion of the activation energy E_{D} for diffusion.

Moreover, the joining of glass devices to glasses and/or to other materials are diffusion-controlled processes which are accompanied by flow. Commonly, the joining procedure is supported by pressure, sometimes even by applying a direct electrical field, for instance during anodic bonding of sodium–boron–silicate glass to silicon.

If two wafers of the same glass are joined, self-diffusion occurs. The process is accelerated by elevated temperatures, at or somewhat above the annealing point T_0. This joining process has to be optimized considering the desired quality of the bonding face and possible deformations of microstructures that can occur around T_0 at the applied pressures to enhance the bond formation. At lower temperatures, around the strain point T_{U}, the glass device could be destroyed because of stress peaks or tilting. In order to keep the deformation of microstructures within an acceptable level the applied bonding pressure should not exceed 0.02 MPa and the temperature not $T = T_0 + 50\,\mathrm{K}$ [190].

As stated above, the ion diffusion can be enhanced by the application of a direct electric field. In most glasses electrical current is conducted by ion movement and, therefore the strong correlation between the diffusion coefficients of ions and electrical conductivity of glasses is not surprising. Any applied electrical field (alternating or direct) acts as driving force which determines the diffusion direction. If the diffusion way of the ions is long, any applied direct current will cause the glass to decompose via electrolysis. However, the decomposition of the glass can be minimized by controlling the temperature, pressure and applied direct electric field. The anodic bonding between glass and silicon will take place via the diffusion of Na^{+} and O^{2-}.

The diffusion length of ions in an applied alternating electric filed is only in the range of ion distances. The diffusion direction changes with the frequency of the alternating field. If the frequency is high enough, the ions will not leave their positions; they will only oscillate around the position at rest, which causes inner friction thereby generating enough heat to melt glass electrically (see also Sect. 3.4.1). In this case, i.e. at elevated temperatures, the diffusion is driven mainly by chemical concentration gradients. Section 3.4.1 deals with technical methods for homogenisation of glass melts. Diffusion processes help the homogenisation of glass melts by reducing chemical composition gradients $\delta\mathrm{c}/\delta\mathrm{x}$ (2.9) and (2.10) in the melt.

It is obvious that the diffusion processes influence almost all glass processing steps ranging from melting to postmanufacturing as well as all the properties of glasses at different temperatures. The higher the temperature the more apparent become the desired or undesired diffusion processes. At $T > T_{\mathrm{g}}$ diffusion as well as flow occur simultaneously, which is beneficial during homogenisation of glass melt or during thermal bonding.

2.3 Enthalpy of Partial Crystallisation

Partial crystallisation of glasses has been described by many authors, see for instance Vogel [538], Scholze [449] and Hinz [225]. The process comprises both steps: the nucleation and the crystal growth.

The free enthalpy G (see also (2.2)) for nucleation of a supercooled glass melt consists of two terms, the volume and the interface term G_v and G_0 (2.11):

$$G = G_\mathrm{v} + G_0. \tag{2.11}$$

G_v describes the formation of the long range order arrangement in the melt, i.e. the nucleation, which is an exothermic process and lowers the free enthalpy; this is counteracted by an increase in interface energy G_0 which is caused by the creation of new boundaries between the amorphous and the long range ordered regions. Both terms may be reduced to specific values, which are expressed for a spherical nucleus with (2.12) and (2.13):

$$G_V = -\frac{4}{3}\pi r^3 \Delta g_\mathrm{v}, \tag{2.12}$$

$$G_0 = 4\pi r^2 \sigma \tag{2.13}$$

where r is radius of the developing nucleus, Δg_v the change of the free volume enthalpy during transformation from the disordered into the ordered state and σ the interfacial tension.

Using (2.12) and (2.13) to complete (2.11) it results in (2.14):

$$G = -\frac{4}{3}\pi r^3 \Delta g_\mathrm{v} + 4\pi r^2 \sigma. \tag{2.14}$$

Δg_v and σ are temperature dependent. Guessing values for Δg_v and σ the following qualitative diagram can be drawn for $G(r)$ at a constant temperature (Fig. 2.2).

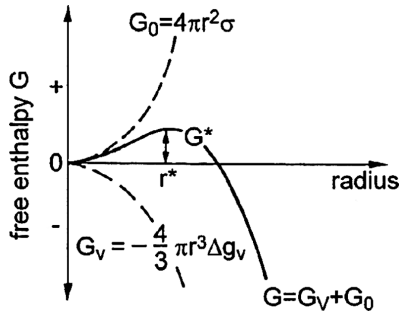

Fig. 2.2. Free enthalpy G of a developing nucleus depending on the actual radius of the ordered volume

The resulting curve for $G(r)$ exhibits a typical maximum. It can be determined in (2.15) by taking the first derivative $\mathrm{d}G(r)/\mathrm{d}r$ and setting it equal to zero:

$$G^* = \frac{16\pi\sigma^3}{3\Delta {g_\mathrm{v}}^2}, \tag{2.15}$$

where G^* is the activation energy for nucleation. The activation energy G^* signifies the amount of energy required to create a nucleus with a critical radius. If the cluster (region of long range ordering) is very small the interfacial energy term will dominate so the cluster is unstable. Only if the size of the cluster exceeds the critical radius r^* (which is equal to $2\sigma/\Delta g_\mathrm{v}$), it becomes stable because the interfacial energy term ceases to dominate and the nucleus has the chance to grow with one's own might. The critical nucleation enthalpy G^* originates from the supercooling of the melt. Nucleation takes only place at $T < T_\mathrm{liqu}$., i.e. via supercooling the melt, see (2.16):

$$G^* \approx \frac{1}{(T_\mathrm{liqu} - T)^2}. \tag{2.16}$$

The critical radius of a nucleus r^* decreases with an increasing degree of supercooling. The principle curve is shown in Fig. 2.3 [538]. The smaller the r^* the more stable nuclei can develop. As consequence the rate of nucleation N depends on the degree of supercooling (T_liqu − T) and on the activation energy G^* for nucleation, see (2.17):

$$N = N_0 \exp -(G^*/kT), \tag{2.17}$$

where N is the rate of nucleation, N_0 is a pre-exponential factor and is equal to N at standard conditions, k the Boltzmann constant and T the absolute temperature.

However, (2.17) is only an approximation. This equation does not account for the kinetic barriers, which are a result of the number of ions, that have

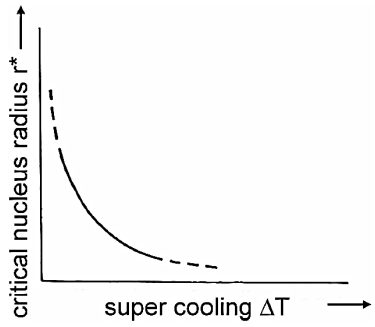

Fig. 2.3. Variation of the critical nucleus radius r^* with the supercooling ΔT of the melt [538]

to be moved and reorganised in a given volume necessary for a crystal with a certain composition to form from a disordered melt (see also Sect. 2.2.2). The process of nucleation is better described by (2.18):

$$J(T) = J_0 \exp - (G^* + E_\mathrm{D})/kT, \tag{2.18}$$

where $J(T)$ is the rate of nucleation including the diffusion of ions, J_0 is equal to J at standard conditions and E_D is activation energy of diffusion. Both quantities, G^* and E_D, depend on temperature, but in an inverse fashion. Therefore, the resulting curve $J(T)$ at $T < T_\mathrm{melt}$ displays a maximum. Annealing a glass at a temperature corresponding to J_max results in the formation of as many nuclei as possible.

The above discussed expressions described the process of homogeneous nucleation. In this case the nucleus forms spontaneously in the supercooled melt and, therefore, the nuclei at which crystallisation eventually occurs are of identical composition with the later crystal. This process has the precondition that nucleation does not occur on bubbles (they are absent) or any other surface and boundaries. On the contrary, heterogeneous nucleation occurs at any surfaces in contact with the melt, such as impurities and the container walls. These nuclei are called heteronuclei. Heteronuclei are already in contact with the glass melt and the boundaries are established, so that only small or no work is required to create them, which means that G^* in (2.18) becomes very small or disappears altogether, which makes it easier for crystals to grow and lowers the temperature range in which crystallisation occurs. This effect is utilised in UV-induced crystallisation in the UV-sensitive glass FS 21 (Sect. 1.2.4). In this special glass Ce^{3+} loses an electron by UV radiation. This one is collected by Ag^+ which changes to a silver atom. This $Ag^{\pm 0}$ has a higher diffusion constant than Ag^+ (see Sect. 2.2.2) and is able to form Ag-clusters at relatively low temperatures. If they are big enough (critical radius) they become nuclei. Ag-nuclei, which act as the substrates for LMS growth, develop at temperatures almost 100 K [365] below the temperature at which normally homogeneous nucleation occurs (around 600°C) [306], if the glass is annealed once more.

The crystal growth can be described by following the arguments which were outlined above, however, in this case the ion transportation processes by diffusion must be considered much more. Frenkel [151] derived in (2.19) an expression for the crystal growth rate KG:

$$KG = A \exp(-1/kT)(E_\mathrm{D} + (CT_0/\lambda\Delta T)), \tag{2.19}$$

where A and C are constants, k is the Boltzmann constant, T the absolute temperature, E_D the activation energy for diffusion, T_0 an equilibrium temperature for the crystal growth, λ the heat of two-dimensional condensation and ΔT the degree of supercooling.

All ions diffusing towards the growing nucleus are deposited at lattice points with the smallest G_0, which explains the dendrite like growth of some

crystals (Fig. 1.41). The diffusion process is driven by chemical and thermal gradients.

The processes occurring during partial crystallisation of glass are not only of importance for the crystallisation of LMS in the UV-radiated regions of UV-structurable glasses (see Sect. 1.2.4), but also for the localised crystallisation of any glasses which can be used to tailor the properties of the material in confined "micro" areas. The partial crystallisation can be induced by means of local heating. The energy supplied has to be large enough to enable crystallisation but should be low enough to avoid the melting of surrounding glass. A focused laser beam is a suitable energy source to induce local crystallisation. The crystallisation should be performed at the temperatures optimal for both, the nucleation and crystal growth. However, temperature control within a glass is rather difficult when using the laser beam. Nevertheless, the energy supplied by the laser must provide the latent heating of the glass up to the crystallisation temperature but also the activation energy for crystallisation. Tammann [512] has found that the curves describing the nucleation process $J(T)$ and the crystal growth $KG(T)$ overlap (Fig. 2.4.).

A glass can be heated to a temperature which enables both processes simultaneously, i.e. nucleation and crystal growth. In order to use laser heating, the laser radiation has to be absorbed by the glass. A laser with a suitable wavelength for a given glass composition has to be chosen. Laser-induced crystallisation can be achieved in various ways; (1) the entire glass sample is heated close to the crystallisation temperature and only the activation energy required to induce crystallisation is supplied by the laser. However, this is technically very challenging. (2) Two lasers are used; an unfocused laser to heat the glass and a focused laser to induce crystallisation. Or (3) only one but well-controlled laser is used. Using laser-induced crystallisation, crystallisation patterns can be *written* by using a microdrived sample stage, which moves relative to the laser.

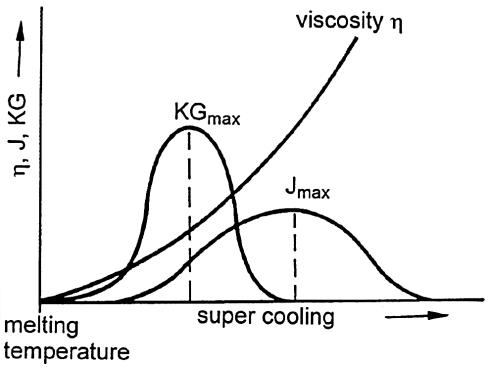

Fig. 2.4. Effect of the degree of supercooling below the melting temperature on the viscosity and rates of nucleation and crystal growth

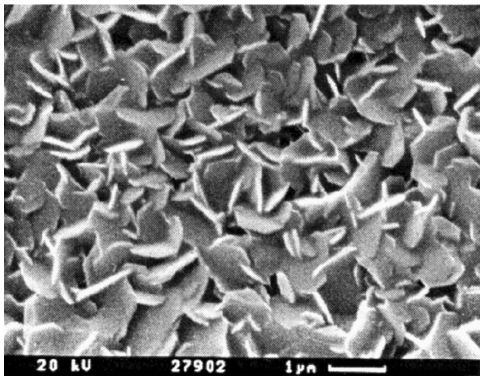

Fig. 2.5. Regions of barium hexaferrite crystals created in a $BaO{-}B_2O_3{-}Fe_2O_3$ glass by laser-induced crystallisation [250]

Figure 2.5 shows an example of patterning a glass using laser-induced crystallisation. The original glass consists of BaO, Fe_2O_3 and B_2O_3 in such amounts that $BaO \cdot 6Fe_2O_3$ (BHF) can crystallise. BHF has hard magnetic properties. By melting and rapid quenching of the melt between two counter rotating, cooled rolls black glassy foils form. The wavelength λ of 1,064 nm of a Nd-YAG laser is strongly absorbed by the glass foils. Magnetic patterns can be *written*, created by laser-induced BHF crystallisation into the glass, if a controlled XYZ-stage is used. The resulting BHF-crystals are single crystalline and, therefore, magnetic as soon as they form.

A similar procedure was made recently by Honma et al. [237]. The authors used glasses in the system $BaO-TiO_2-GeO_2-SiO_2$, which are suitable for fresnoite-type crystallisation. The applied heat source was a cw-YAG (yttrium–aluminum–garnet) laser.

2.4 Enthalpy of Melting and Evaporation

Glasses can be microstructured also by means of ablation. Material is heated until it evaporates. Laser radiation can be used to supply enough heat to vaporise glass. Since glasses do not possess long range order (crystalline structures), they have no well-defined melting and evaporating temperatures, i.e. glasses do not undergo first-order phase transitions. Instead of a well-defined melting point, the viscosity of a glass changes continuously as function of temperature (Fig. 2.1). The slope of the viscosity–temperature curve decreases with increasing temperature. *Practical* experiences indicate that a glass is homogeneously melted without bubbles if it has a viscosity of about 10 Pa s. The slope of the viscosity–temperature curve of a sodium lime silicate glass (Fig. 2.1) at this temperature is only 180 kJ mol^{-1}, which is much lower than the chemical binding energy $B \approx 420$ kJ mol^{-1} at room

temperature. The apparent discrepancy between both values is explained by the slow continuous softening of the glass in the whole temperature range above the transformation temperature. Therefore, it is not possible to define the melting enthalpy; instead the activation energy of viscous flow at different temperatures has to be estimated.

The same holds true for the evaporation enthalpy of glasses. A precise value for the evaporation enthalpy of a one-component glass, such as quartz glass (SiO_2) can be defined. However, already for a two-component glass, such as Na_2O–SiO_2 or K_2O–SiO_2, the evaporation enthalpy cannot be clearly determined anymore because of the presence of different types of chemical bonds, such as Na–O and Si–O (see Sect. 1.1.3). Na_2O evaporates at lower temperatures than SiO_2. Nevertheless, Kröger and Sörström [312] published evaporation enthalpies E_E for a binary Na_2O–SiO_2 glass of $E_E = 290\,\mathrm{kJ\ mol^{-1}}$ and for ternary Na_2O–CaO–SiO_2 glasses of $E_E = 355$–$545\,\mathrm{kJ\ mol^{-1}}$. In case of the ternary Na_2O–CaO–SiO_2 glass the evaporation enthalpies exceed the chemical binding energy at room temperature. The most chemical bindings are broken; the glass evaporates.

2.5 Redox Equilibria

The redox equilibrium, see (2.20)

$$Ag^{+} + Ce^{3+} \xrightarrow{h\cdot\nu} Ag^{0} + Ce^{4+} \tag{2.20}$$

was already discussed in Sect. 1.2.4. If a glass contains multivalent elements as main components or as dopants the possibility that redox reactions occur has to be considered. If such reaction occurs within a glass it will affect all its properties.

The redox equilibria are of great importance for the following processes:

- Heterogeneous nucleation in photostructurable glasses
- Electrical conductivity/resistance of glasses containing lead oxide
- The colouring of glasses
- Refining processes, see also Sect. 3.2.1

Whether or not redox reactions can occur in glasses depends in the first instance on the valency of the ions present but is strongly influenced by the:

- Coordination number of the multivalent element (see Sect. 1.1)
- Neighbouring coordination polyhedra of the polyvalent ions [538]
- The melting temperature and residence time of the melt
- Chosen raw materials to produce the glass [365]
- Occasionally the addition of reducing or oxidizing agents to the melt
- Relative humidity of the atmosphere, the presence of crystal water in the raw materials and the water content of the batch

It is also obvious that all of the above are interrelated. Detailed reviews of redox processes in glasses can be found in the literature [29, 43, 371, 414, 538].

Because of interactions between various redox pairs it is rather difficult to understand the redox processes occurring in glasses. This requires specially designed experiments of well-defined glass compositions, see also Rüssel [433]. Redox processes in glasses are very difficult to generalise. It is virtually impossible to transfer experiences from one glass composition to another.

http://www.springer.com/978-3-540-49888-9

Microstructuring of Glasses
Hülsenberg, D.; Harnisch, A.; Bismarck, A.
2008, XX, 326 p.,
ISBN: 978-3-540-49888-9